



## **MODEL VERIFICATION AND PERCUSSION SOUND CHARACTERISTICS OF METALLOPHONE WITH CHORD SOUND**

Bor-Tsuen Wang, and Xiao-Ming Jian

*Department of Mechanical Engineering, National Pingtung University of Science and Technology, Pingtung, 91201, Taiwan  
e-mail: wangbt@mail.npust.edu.tw*

The metallophone is a common percussion instrument. The percussion sound of the metallophone is strongly related to the structural vibration modes. This paper presents the new design geometry of metallophone plate that can produce the C major chord sound. The finite element (FE) model for the metallophone plate is constructed to perform the theoretical modal analysis so as to obtain natural frequencies and mode shapes. The experimental modal analysis (EMA) is then carried out on the metallophone plate to determine the structural modal parameters. Base on the experimental results the FE model can be verified and further applied to design modification analysis. The percussion sound of the specially designed chord metallophone is also measured and shown its chord sound characteristics. The new designed metallophone that can produce chord sound is a brand new concept for the percussion instrument. The integration of FEA and EMA techniques is shown effective for the design of percussion instruments.

### **1. Introduction**

The metallophone is one of the percussion instruments that are tuned metal bars struck by a mallet to make sound. The metallophone is commonly played in musical performance and has been developed various kinds in different countries [1]. The percussion sound of metallophone or any percussion instrument is strongly related to the structural vibration characteristics that are affected by the geometrical shape and size as well as materials. Rossing [2] presented the acoustical principle of various types of percussion instruments.

The study of percussion sound characteristics is of interest. Wang and Lin [3] conducted experimental modal analysis (EMA) on a simple type of metallophone bar with rectangle shape to characterize the modal properties. They [4] also showed the sound and vibration correlation for the metallophone bar. The percussion sound is mainly dominated by the structural vibration modes and

affected by the struck location and even the striking stick materials. Wang *et al.* [5] and Wang and Chen [6] studied the sound and vibration characteristics of two types of copper gongs, respectively, that are frequently used in Taiwan for festival events. The special feature of gong structure is the circular shape made of thin copper plate.

The xylophone, another frequently seen percussion instrument, is made of wood materials. Bork [7] developed mathematical beam model to tune the xylophone bar to improve the inharmonic sound characteristics. Bretos *et al.* [8] applied finite element (FE) method in analyzing and comparing the modal frequencies for two types of undercuts of xylophone bars and verified by frequency measurement. Bretos *et al.* [9] completed the previous work with more detail studies on mode shape characteristics of xylophone bar and the variation of material and size effects. Chaigne and Doutaut [10] formulated the theoretical model including the mallet effect on simulating the transient dynamic response for xylophone bars. Doutaut *et al.* [11] further extended the numerical model to include the resonator effect under the xylophone bar. Wang and Liao [12] adopted the integration of FEA and EMA techniques to perform model verification of a xylophone bar. Other percussion instruments such as bells [13-15] or kettledrum [16] were also studied.

This work will present the use of FEA and EMA techniques on the special designed metallophone plate that can produce C major chord sound. The FE model of the metallophone plate is constructed for analytical solution of modal parameters that are verified in comparison to EMA results. The validated FE model can then be used for further structural modification. The sound radiation characteristics related to the structural vibration modal properties are also discussed and shown the unique spectrum consisting of the triad chord sound. This work leads for the idea of structural shape design for percussion instruments.

## 2. Model verification of metallophone plate

Figure 1(a) shows the newly designed metallophone plate that has the percussion sound characteristics of C major chord. Table 1 reveals the musical notes from C<sub>6</sub> to C<sub>7</sub> and their corresponding frequencies. The C major triad chord consists of C, E and G. This section discusses the main idea about model verification to validate the analytical model of metallophone plate constructed by finite element software.

Figure 2 is the flow chart of model verification on the metallophone plate. The FE model of the metallophone plate is first constructed and performed modal analysis to obtain the structural modal properties, i.e. natural frequencies and mode shapes as well as the frequency response function (FRF) by harmonic response analysis. On the other hand, experimental modal analysis or so called modal testing is carried out by measuring the structural FRFs that will be processed to determine the modal parameters for the real structure. Then, both FEA and EMA results can be compared to validate the FE model base on the experimental data by the correction of system parameters. The equivalent FE model can be validated if modal parameters from both FEA and EMA can agree to each others.

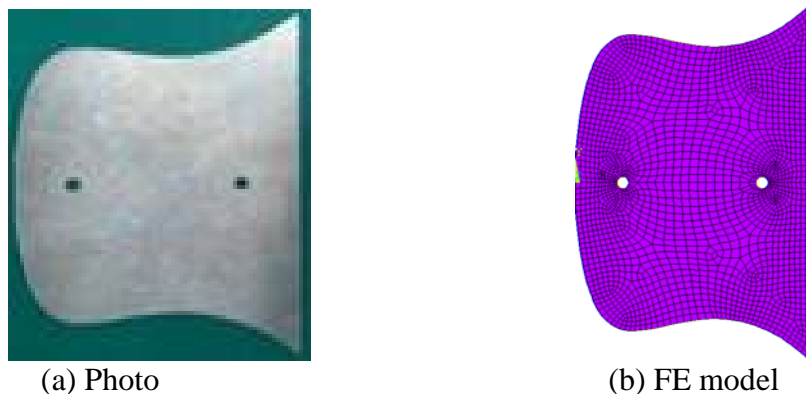


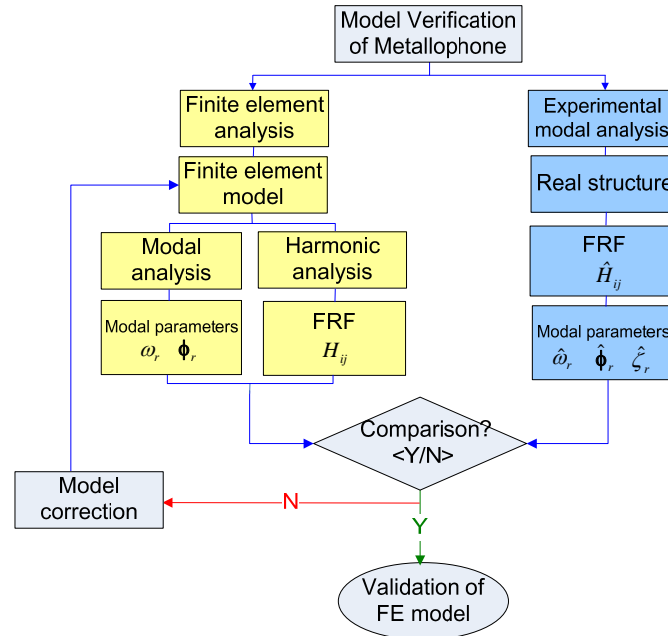
Figure 1. metallophone plate.

**Table 1. Musical notes and corresponding frequencies.**

Musical note	<b>C6</b>	D6	<b>E6</b>	F6	<b>G6</b>	A6	B6	C7
Frequency (Hz)	<b>1046.5</b>	1174.6	<b>1318.5</b>	1396.9	<b>1568.0</b>	1760.0	1975.5	2093.0

**Table 2. Material properties of metallophone plate.**

Young's modulus (GPa)	Density (kg/m <sup>3</sup> )	Poisson ratio
192.95	7782.92	0.27



**Figure 2.** flow chart for model verification of metallophone plate.

## 2.1 Finite element analysis

This work adopts the commercial FE code, ANSYS, to build the FE model of the metallophone plate. Figure 1(b) reveals the mesh of the FE model, and Table 2 shows the material properties of the metallophone plate after calibration via model verification procedure. The linear quadrilateral shell element (SHELL63) can be used to construct the model because the plate is relatively thin. The element size is generally about 3mm in width. In corresponding to EMA, the metallophone plate is suspended as shown in Figure 3(a), and thus free boundary is assumed. For modal analysis, no loading condition is required. The theoretical natural frequencies ( $f_r$ ) and mode shapes ( $\phi_r$ ) can be obtained. The unit point force is applied at the struck location by the impact hammer in accordance with EMA for harmonic response analysis to obtain system FRF ( $H_{ij}$ ).

## 2.2 Experimental modal analysis

Figure 3(a) is the experimental setup for EMA on the metallophone plate, and Figure 3(b) shows the 30 test grid points on the plate. The mini impact hammer is applied as the actuator to excite the structure and roving over the grid points, while the accelerometer is fixed at point 2 to measure the acceleration. Therefore, the experimental FRF,  $\hat{H}_{ij}$ , between the acceleration at  $i$ -th point and the force input at  $j$ -th point can be obtained and used to perform curve fitting so as to determine the experimental modal parameters, including natural frequencies ( $\hat{f}_r$ ), mode shapes ( $\hat{\phi}_r$ ) and modal damping ratios ( $\hat{\zeta}_r$ ). In addition to the use of accelerometer as the sensor, this work also applies the microphone fixed at the direction of 45° and 20cm away from the centre of the metallo-

phone plate by roving the impact hammer. The two independent EMA experiments are performed to compare the extracted modal parameters. Since the actuator is roving and the sensor is fixed, the actuator mode shape can be extracted from the measured FRFs [17]. Here, the impact hammer is the point type force, and thus the displacement mode shape for each mode can be obtained.

The percussion sound of the metallophone plate is also measured by striking on different locations of the plate with a mallet. The sound spectrum is recorded and interpreted to show the sound characteristics of the metallophone.

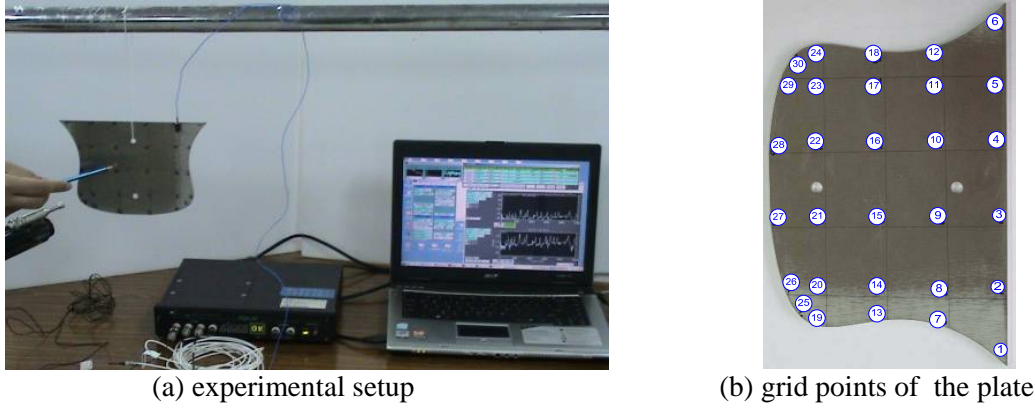


Figure 3. Experimental setup for modal testing of metallophone plate.

### 3. Results and discussions

This section will show the model verification results of the metallophone plate by combining the FEA and EMA techniques to validate the FE model of the plate. The percussion sound spectrum of the metallophone plate will also be presented.

#### 3.1 Model verification of metallophone

Figure 4(a) and 4(b) show the FRFs obtained from EMA via the accelerometer and microphone, respectively. In Figure 4(a), the solid line denotes the measured FRF, and the dashed line is the synthesized FRF obtained from the extracted modal parameters. That both FRFs agree very well indicates the correctness on the curve fitting procedure. The long dashed line is the theoretical FRF obtained from FEA that generally agrees well with experimental one, i.e. the analytical FE model of the metallophone plate is well simulated. For the microphone as the sensor as shown in Figure 4(b), the experimental FRF is not so smooth due to the background noise resulting in the low response of sound emission from the metallophone plate, in particular at non-resonance regions. However, the resonant frequencies of the metallophone can still be well identified and thus the FRFs can also be used for modal parameter extraction. As one can see the synthesized FRF from the EMA via microphone also match well with the experimental one. Note that the sound radiation simulation is not conducted in this work.

Table 3 shows the comparison of natural frequencies and modal damping ratios obtained from FEA and both EMA results via the accelerometer and microphone, respectively, for natural modes within 10,000Hz frequency range. The error percentages of natural frequencies between FEA and EMA are generally within 2% except a few modes as bolded in Table 3. The modal assurance criterion (MAC) is defined as follows:

$$MAC(\hat{\phi}_r, \phi_s) = \frac{|\hat{\phi}_r^T \phi_s|^2}{(\hat{\phi}_r^T \hat{\phi}_r^*) (\phi_s^T \phi_s^*)}, \quad r = 1, 2, \dots, n, \quad s = 1, 2, \dots, n \dots \quad (1)$$

The *MAC* is a scale to compare the similarity of two vectors. If *MAC* values are close to 1, the two vectors match perfectly in scale. If *MAC* values are zero, the two vectors are orthogonal. As one can observe in Table 3 as well as Table 4 showing those theoretical and experimental mode shapes for the first 6 modes, the *MAC* values between the mode shape vectors obtained from FEA ( $\phi_r$ ) and EMA ( $\hat{\phi}_r$ ) are mostly above 0.8 and this indicates the physical agreement of mode shape characteristics. The types of modes are also indicated such as (x,y)=(2,2), i.e. revealed as the typical plate mode shape. The modal damping ratios obtained from both EMA experiments are about the same. It is noted that the averaged modal damping ratio for all modes is determined and used as the constant modal damping ratio in the FE model to determine theoretical FRF as shown in Figure 4(a).

In summary, the model verification of the metallophone plate is performed to validate the analytical FE model base on the modal data comparison. The modal characteristics of the metallophone plate can be well interpreted and match to each others between FEA and EMA. The use of microphone as the sensor for EMA is also shown effectively. Since the microphone is a type of non-contact sensor, the sensor mass effect does not exist in contrary to the accelerometer.

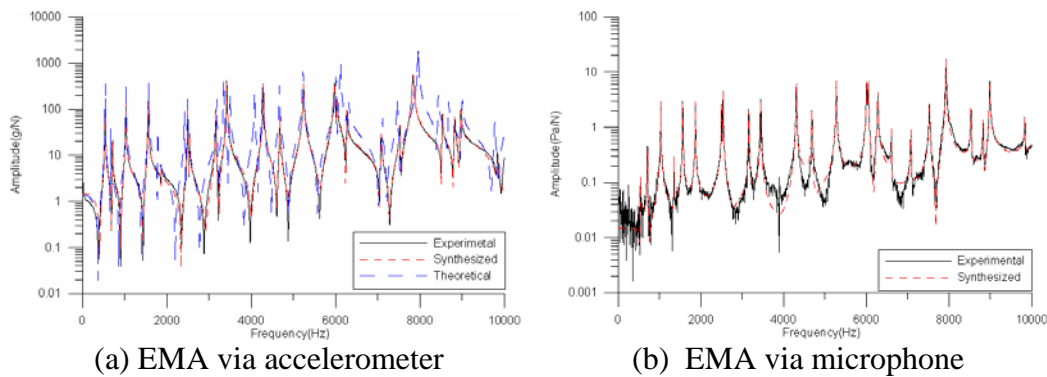


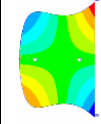
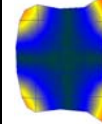
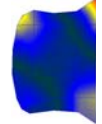
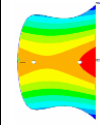
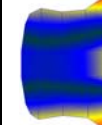
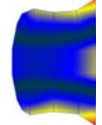
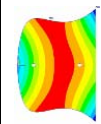
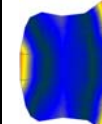

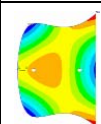
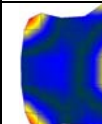
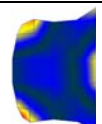
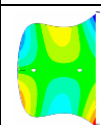
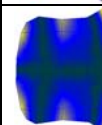
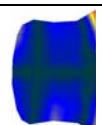
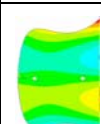
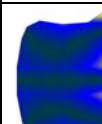
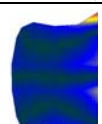
Figure 4. Frequency response function (FRF) of  $H_{2,2}$ .

Table 3. Comparison of modal parameters between FEA and EMA.

Mode	Type of mode	FEA (Hz)	EMA via acc. (Hz)	Diff. (Hz)	Error (%)	MAC	Damping ratio (%)	EMA via mic. (Hz)	Diff. (Hz)	Error (%)	MAC	Damping ratio (%)
1	(2,2)	536.99	537.5	-0.5	-0.095	0.947	0.435	540.6	-3.6	-0.668	0.748	0.416
2	(1,3)	664.98	712.5	-47.5	-6.669	0.824	0.330	709.4	-44.4	-6.262	0.829	0.326
3	(3,1)	1035.2	1028.1	7.1	0.688	0.874	0.244	1031.3	3.9	0.378	0.866	0.246
4	(2,3)	1322.8	1346.9	-24.1	-1.787	0.959	0.160	1350.0	-27.2	-2.015	0.949	0.175
5	(3,2)	1572.8	1559.4	13.4	0.861	0.910	0.162	1562.5	10.3	0.659	0.859	0.152
6	(1,4)	1784.7	1868.8	-84.1	-4.498	0.892	0.136	1868.8	-84.1	-4.500	0.895	0.132
7(E8)	(3,3)	2417.2	2540.6	-123.4	-4.858	0.867	0.107	2500.0	-82.8	-3.312	0.826	0.104
8(E7)	(2,4)	2492.3	2496.9	-4.6	-0.183	0.932	0.107	2543.8	-51.5	-2.025	0.799	0.105
9	(4,1)	3185.0	3156.3	28.8	0.911	0.875	0.109	3162.5	22.5	0.711	0.504	0.096
*10	(2,4)	3354.0	3421.9	-67.9	-1.984	0.844	0.097	3453.1	-99.1	-2.870	0.604	0.107
11	(4,2)	3498.2	-	-	-	-	-	-	-	-	-	-
12	(2,5)	4081.2	-	-	-	-	-	-	-	-	-	-
13	(3,4)	4264.7	4287.5	-22.8	-0.532	0.444	0.089	4312.5	-47.8	-1.108	0.233	0.080
14	(4,3)	4668.1	4681.3	-13.1	-0.281	0.911	0.105	4687.5	-19.4	-0.414	0.368	0.093
15	(3,6)	5226.2	5240.6	-14.4	-0.275	0.914	0.126	5257.0	-30.8	-0.586	0.659	0.082
16	(4,4)	6010.5	5978.1	32.4	0.542	0.328	0.157	6012.5	-2.0	-0.033	0.558	0.093
17	(※)	6114.3	6031.3	83.1	1.377	0.497	0.091	6053.1	61.2	1.011	0.547	0.066
18	(5,3)	6246.2	6271.9	-25.7	-0.409	0.829	0.096	6281.3	-35.1	-0.559	0.570	0.095
19	(4,6)	6312.6	-	-	-	-	-	-	-	-	-	-
20	(4,7)	7115.5	7078.1	37.4	0.528	0.789	0.095	7081.3	34.2	0.483	0.434	0.082
21	(5,4)	7463.3	7525.0	-61.7	-0.820	0.834	0.106	7528.1	-64.8	-0.861	0.238	0.091
22	(5,7)	7959.3	7837.5	121.8	1.554	0.874	0.160	7931.3	28.0	0.353	0.398	0.051
*23	(4,6)	8432.5	8534.4	-101.9	-1.194	0.851	0.081	8537.5	-105.0	-1.230	0.347	0.062
24	(3,7)	8676.0	8825.0	-149.0	-1.688	0.732	0.091	8828.1	-152.1	-1.723	0.208	0.069
*25	(5,4)	9006.5	8971.9	34.6	0.386	0.712	0.120	8987.5	19.0	0.211	0.456	0.068
*26	(3,4)	9774.8	-	-	-	-	-	-	-	-	-	-
27	(6,1)	10119.0	9834.4	284.6	2.894	0.374	0.0967	9834.4	284.6	2.894	0.297	0.064



**Table 4. Comparison of mode shapes between FEA and EMA.**

Target Freq. (Hz)	mode	Type of mode shape	FEA		EMA via acc.		EMA via mic.	
			Natural Freq. (Hz)	Mode shape	Natural Freq. (Hz)	Mode shape	Natural Freq. (Hz)	Mode shape
-	1	(2,2)	536.99		537.5		540.6	
-	2	(1,3)	664.98		712.5		709.4	
1046.5	3	(3,1)	1035.2		1028.1		1031.3	
1318.5	4	(2,3)	1322.8		1346.9		1350.0	
1568.0	5	(3,2)	1572.8		1559.4		1562.5	
-	6	(1,4)	1784.7		1868.8		1868.8	

### 3.2 Sound characteristics of metallophone

Figure 5 reveals the nodal lines of mode shapes of the metallophone plate for modes 1-5. The numbers at the edge of the plate are the corresponding mode number. The physical insight of the nodal lines is where there is no vibration or in still in the corresponding modal response. Table 5 shows the measured sound spectrum for using the mallet striking at the points 1 and 3, respectively, and Table 6 shows the peak frequencies and their sound pressure levels (dB). Some observations are discussed as follows:

- For the struck point 1, as shown in Figure 5, where is right at the nodal lines of modes 1 and 2, as expected the first and second modes can not be excited, and therefore the sound spectrum only reveals the peak resonant frequencies at modes 3-6 as indicated in Table 5.
- When the mallet is struck at point 3, where is the cross point of the nodal lines for modes 1, 3, 5 and 6, the peak resonances on the sound spectrum are modes 2 and 4. The hearing sound will be only the two modal frequencies.
- The innovation of the metallophone plate is that the modal frequencies of modes 3, 4 and 5 are nearly corresponding to the C major chord as the bolded musical notes shown in Table 2. Therefore, this metallophone plate can produce C major chord sound characteristics for struck at point 1 as well as point 2.
- Different struck points on the metallophone plate will generate different percussion sounds base on the mode shape characteristics. With the proper shape design of the metallophone

plate to tune the modal frequencies and the selection of struck points, the special objective oriented design of the metallophone plate can be made.

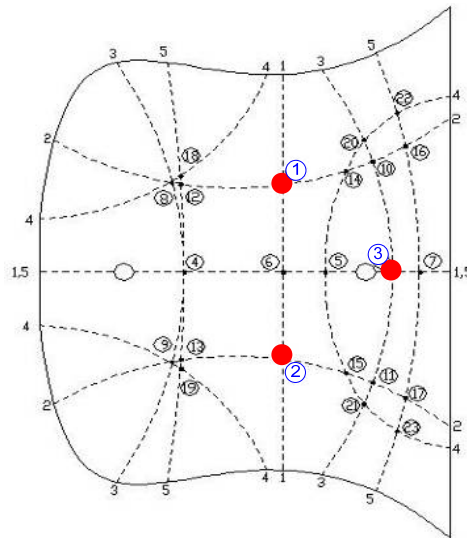


Figure 5. Overlap of nodal lines for modes 1-5.

Table 5. Percussion sound spectrum of metallophone plate.

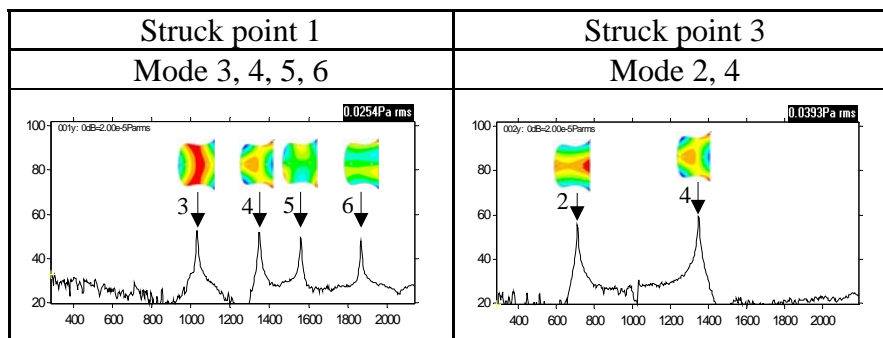


Table 6. Percussion sound pressure levels and frequencies of metallophone plate.

Struck point	1		3	
mode	$f_r$ (Hz)	dB	$f_r$ (Hz)	dB
1	---	---	---	---
2	---	---	709.375	55.368
3	1031.250	52.859	---	---
4	1346.875	51.718	1346.875	59.493
5	1559.375	49.384	---	---
6	1868.750	47.730	---	---

#### 4. Conclusions

This work presents the model verification of a special designed metallophone plate that can produce C major chord sound. The integration of FEA and EMA techniques is applied to validate the FE model of metallophone plate and shown promising. The validated FE model can be further used to perform structural modification for particular shape design of metallophone. Besides the traditional EMA by using the accelerometer as the sensor, the microphone is also shown feasible for modal testing and effective. The advantage of the microphone over the accelerometer is the non-contact type of sensor and lack of mass effect on the test structure, though the background noise has to be well controlled. The percussion sound spectra of the metallophone are also studied to show its

special chord sound characteristics depending on the struck location. This work develops the methodology in both analytical and experimental approaches for percussion instrument design and analysis. The systematic approach does provide the tools in analysing and designing the musical instruments, in particular for the metallophone revealed in this work.

## 5. Acknowledgement

The authors are grateful for the financial support of this work under the contract number: NSC98-2221-E-020-009 from National Science Council, Taiwan.

## REFERENCES

- [1] <http://en.wikipedia.org/wiki/Metallophone>. (accessed on 03/19/2010)
- [2] T.D. Rossing, "Acoustics of percussion instruments: recent progress," *Acoustical Science and Technology* **22** (3), 177-188 (2001).
- [3] B.T. Wang and Y.S. Lin, "Comparison of experimental modal analysis on metal bar of metallophone by using accelerometer and microphone as sensors," *Proceedings of the 31st National Conference on Theoretical and Applied Mechanics*, Kaohsiung, Taiwan, 2007, Paper No.: H31. (In Chinese)
- [4] B.T. Wang and Y.S. Lin, "Vibration and sound correlation study for a metal bar of metallophone," *Proceedings of the 20th Conference of Acoustical Society of Republic of China*, Taipei, Taiwan, 2007, Paper No.: C5. (In Chinese)
- [5] B.T. Wang, Y.S. Lee and Z.W. Chang, "The study of vibration and sound characteristics of copper gong," *The Tenth National Conference on the Society of Sound and Vibration*, 2002, pp. 245-252. (In Chinese)
- [6] B.T. Wang and S.C. Chen, "Sound and vibration characteristic discussion the gong navel form copper gong," *Proceedings of the 21st Conference of Acoustical Society of Republic of China*, Taipei, Taiwan, 2008, Paper No.: A1-4. (In Chinese)
- [7] I. Bork, "Practical tuning of xylophone bars and resonators," *Applied Acoustics* **46**, 103-127 (1995).
- [8] J. Bretos, C. Santamaria and J. Alonso Moral, "Tuning process of xylophone and marimba bars analyzed by finite element modelling and experimental measurements," *Journal of the Acoustical Society of America* **102**(6), 3815-3816 (1997).
- [9] J. Bretos, C. Santamaria and J.A. Moral, "Finite element analysis and experimental measurements of natural eigenmodes and random responses of wooden bars used in musical instruments," *Applied Acoustics* **56**, 141-156 (1999).
- [10] A. Chaigne and V. Doutaut, "Numerical simulations of xylophones. I. time-domain modelling of the vibrating bars," *Journal of the Acoustical Society of America* **101**(1), 539-557 (1997).
- [11] V. Doutaut, D. Matignon and A. Chaigne, "Numerical simulations of xylophones. II. time-domain modelling of the resonator and of the radiated sound pressure," *Journal of the Acoustical Society of America* **104**(3), 1633-1647 (1998).
- [12] B.T. Wang and W.T. Liao, "Experimental modal analysis and model verification of a xylophone bar," *The 17th National Conference on Sound and Vibration*, Taipei, 2009, Paper No.: B-06. (in Chinese)
- [13] T.D. Rossing and H. J. Sathoff, "Modes of vibration and sound radiation from tuned handbells," *Journal of the Acoustical Society of America* **68**(6), 1600-1607 (1980)
- [14] M. Jing, "A theoretical study of the vibration and acoustics of ancient Chinese bells," *Journal of the Acoustical Society of America* **114**(3), 1622-1628 (2003).
- [15] N. McLachlan, "The application of new analyses and design methods to musical bells," *75th Acoustical Society of America Conference*, New York, 2004, pp. 1-8.
- [16] L. Rhaouti, A. Chaigne and P. Joly, "Time-domain modelling and numerical simulation of a kettledrum," *Journal of the Acoustical Society of America* **105**(6), 3545-3562 (1999).
- [17] B.T. Wang, "Vibration analysis of a continuous system subject to generic forms of actuation forces and sensing devices," *Journal of Sound and Vibration* **319**, 1222-1251 (2009).